catalysts

MDPI

Review

The Role of Sulfated Materials for Biodiesel Production from Cheap Raw Materials

Brandon Lowe, Jabbar Gardy * and Ali Hassanpour

School of Chemical and Process Engineering, Faculty of Engineering and Physical Sciences, University of Leeds, Leeds LS2 9JT, UK; pmblo@leeds.ac.uk (B.L.); a.hassanpour@leeds.ac.uk (A.H.)
* Correspondence: j.gardy@leeds.ac.uk; Tel.: +44-73-9233-3760

Abstract: There is an urgent need to reduce global greenhouse gas emissions, yet to date the decarbonization of the transportation industry has been slow and of particular difficulty. While fossil fuel replacements such as biodiesel may aid the transition to a less polluting society, production at the industrial scales required is currently heavily dependent on chemical catalysis. Conventional two-step homogenous routes require the challenging separation of catalyst from the obtained product; however, heterogenous solid catalysts bring new considerations such as material stability, surface area, porosity, deactivation effects, and reduced reactivities under mild conditions. Nanomaterials present an attractive solution, offering the high reactivity of homogenous catalysts without complex recyclability issues. Slightly less reactive, acidic sulfated nanomaterials may also demonstrate greater stability to feedstock impurity, extending lifetime and improved versatility to a range of starting feeds. There remains, however, much work to be done in demonstrating the full-scale feasibility of such catalysts. This review explores recent developments over time in acidic sulfated nanocatalysis for biodiesel production, with particular focus on metal oxides, magnetic nanoparticles, silica-supported nanomaterials, and acidic carbon nanocatalysts. Included are various summaries of current progress in the literature, as well as recommendations for future research.

Keywords: biodiesel; magnetic nanoparticle; sulfated nanoparticle; transesterification; esterification/transesterification; waste cooking oil

Citation: Lowe, B.; Gardy, J.; Hassanpour, A. The Role of Sulfated Materials for Biodiesel Production from Cheap, Raw Materials. *Catalysts* **2022**, *12*, 223. https://doi.org/10.3390/catal12020223

Academic Editor: Antonella Gervasini

Received: 26 January 2022
Accepted: 14 February 2022
Published: 16 February 2022

1. Introduction

The recent COP26 climate change conference [1] reiterated the pressing need to dramatically reduce greenhouse gas (GHG) emissions. Road transportation accounts for more than 10% of global contributions and such emissions are reportedly rising faster than any other sector in society [2]. There is a clear need for a rapid transition away from traditional fossil fuel-powered internal combustion vehicles. While electric vehicle technology continues to receive investment and shows promise [3], a significant population of legacy vehicles will likely continue to be needed for the foreseeable future, especially in less economically developed countries where electrical grids are less developed. Biodiesel can be used either as a direct replacement into existing engine technology, or mixed in with traditional petroleum as a biodiesel blend [4,5]. Although not truly carbon neutral when considering the complete lifecycle, biodiesel does reduce vehicle GHG emissions, as well as being cleaner burning and safer to use than petroleum alone [6]. A wide range of feedstocks can be used for biodiesel production, with each type of feedstock introducing various social, economic, environmental, and technical challenges.

Vegetable oils and animal fats are typically used in food production, and therefore usage in the fuel industry would encourage undesirable competition, referred to as the issue of "food vs. fuel" [7]. Other non-edible, algal or waste cooking oils (WCO) could be used; however, issues of affordability and ensuring sufficient supply to meet an ever-

growing demand would need to be addressed [8,9]. Impure feedstock such as WCO could potentially be both cheap and plentiful in supply, although high water and free fatty acid (FFA) content [10,11] requires resilient catalysts.

Biodiesel is predominantly produced from catalytic transesterification and esterification reactions [12,13], as illustrated in Figure 1. These reactions require the use of a catalyst to ensure sufficiently fast reaction kinetics at moderate temperatures. The fat or oil feedstock contains a source of triglycerides and FFA, which reacts with methanol to produce a mixture of fatty acid methyl esters (FAME) [14]. After the purification and removal of glycerol byproduct, vehicle-ready biodiesel is obtained. Most modern biorefineries currently utilize a two-step homogenous catalysis approach, where esterification is first performed using an acid catalyst such as sulfuric acid, followed by transesterification using a base such as sodium hydroxide [15]. The addition of acid in the first step ensures FFA is reacted prior to the addition of the base catalyst, avoiding the undesirable production of soap via saponification [13,16], and the deactivation of the more reactive base catalyst. Unfortunately, the separation of homogenous catalyst post-reaction is often challenging, expensive, and requires neutralization of the biodiesel to prevent engine corrosion [17–19]. While solid heterogenous catalysts can be separated more easily from the biodiesel product, new engineering challenges may be faced including lower reactivity, reduced surface area [20], pore blocking [21], and site instability over repeated usage [22,23]. The cost of catalyst regeneration and replacement of spent material must also be considered.

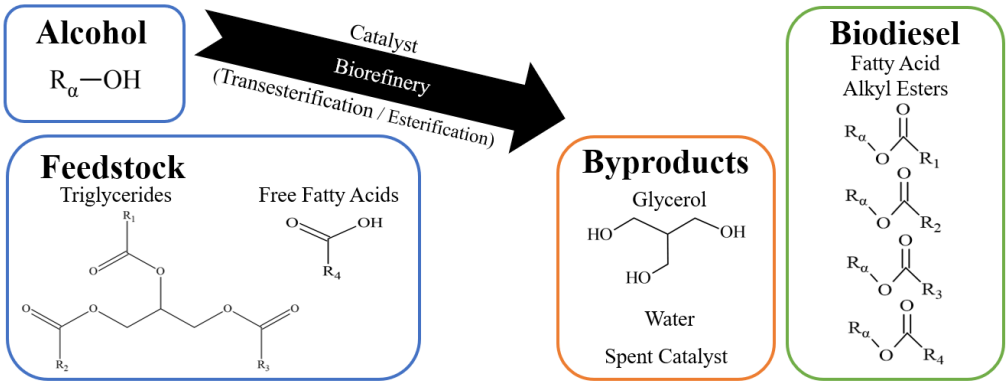

Figure 1. Catalytic production of biodiesel.

The field of nanotechnology is an exciting area of active research that offers an interesting alternative to traditional approaches. By developing a nanocatalyst, it is possible to combine both high reactivities observed in homogenous catalysis with the ease of separability observed with heterogenous materials [24]. Depending on the intended application, nanocatalysts can be designed to exhibit acidic, basic, or combined bifunctional activity through the inclusion of Lewis acidic or basic species. Furthermore, post-synthesis functionalization can be performed to introduce new functional groups onto the catalyst surface, such as Bronsted acidic sulfate groups. The inclusion of magnetic species can also achieve rapid separation with improved recovery via the external field [25].

Sulfated nanomaterials have seen a wide range of applications, from energy storage [26], medicine [27], and pollution control [28] to demonstrating the ability to readily catalyse a range of industrially important petrochemical reactions, including transesterification, esterification, and hydrocracking [29]. The use of sulfated nanocatalysts for the conversion of waste feedstocks into biodiesel, or through the hydrocracking and isomerization upgrade route into sustainable aviation fuels [30,31], could be more desirable over current industrial processes through achieving similar reactivities at reduced reaction temperatures and pressures. While non-catalytic routes for biodiesel production are also under development, such as supercritical methanol [32–36], the BIOX process [37], ther-

mal cracking, and pyrolysis routes, existing state of the art biorefineries are predominantly designed for homogenous catalysis. Sulfated nanocatalysts could be utilised in existing facilities without significant redesign, facilitating both improved separability and high reaction rates at mild conditions. Non catalytic routes, meanwhile, would likely be incompatible with existing biorefinery plants, and may still be less environmentally sustainable overall. Although basic nanocatalysts may demonstrate superior reactivity, acidic nanoscale catalysts can effectively make use of a wider variety of impure feedstocks both cheap and readily available, such as WCO [38]. Moreover, biorefineries wishing to directly react feedstock without pre-treatment steps could utilize such acidic nanocatalysts, further reducing process complexity. For these reasons, this review will primarily focus on sulfated solid acid nanocatalysis. A range of acidic catalysts will be explored, including some bifunctional materials where sulfated acid sites are of particular interest. Progress and developments over time are summarized chronologically, alongside suggestions for future work to address remaining challenges that will need to be solved before commercial use is seen at the industrial scale.

2. Solid Acid Nanomaterials

2.1. Types of Solid Acids

A diverse range of solid acid nanocatalysts have been developed for biodiesel production, as summarized in Figure 2. Acidity is often classified into Lewis or Brønsted behaviour, with reactions initiating via electron pair acceptance or proton donation, respectively. The type of acidity present is influential, since Lewis acids tend to favour triglyceride transesterification [39], whilst Brønsted sites can better handle FFA impurities by favouring the esterification pathway. For Lewis acidic metal oxides, catalysis can occur via the positively charged metal cation accepting an electron pair from an alcohol to produce a reactive alkoxide intermediate [40]. The presence of Brønsted groups in sulfated metal oxides can instead initiate reaction through protonation of the FFA carbonyl group.

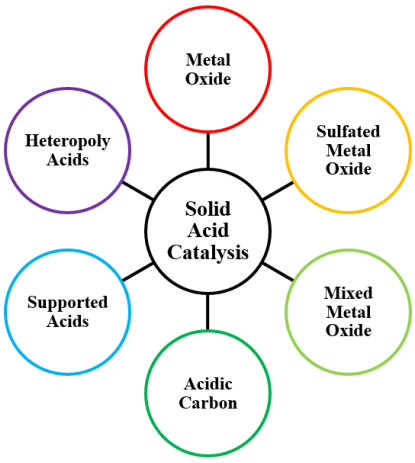

Figure 2. Types of solid acid nanomaterials.

A schematic of these sites on the solid surface and the initial mechanism step is included in Figure 3. Addition of different metals can further enhance catalytic performance by improving surface area, porosity, stability, or reactivity. Such mixed metal oxide materials can even be designed to be bifunctional, with acid sites helping to esterify FFA and protecting base sites from undesirable saponification and deactivation [41]. Carbon nanomaterials and inert supports, including porous silica and zeolites, can also be acid functionalized to catalyse biodiesel production. Additionally, insoluble or support immobilized heteropoly acids (HPA) have been developed, such as Keggin $[XM_{12}O_{40}]^{n-}$ structures [42] of central atom X surrounded by M atoms.

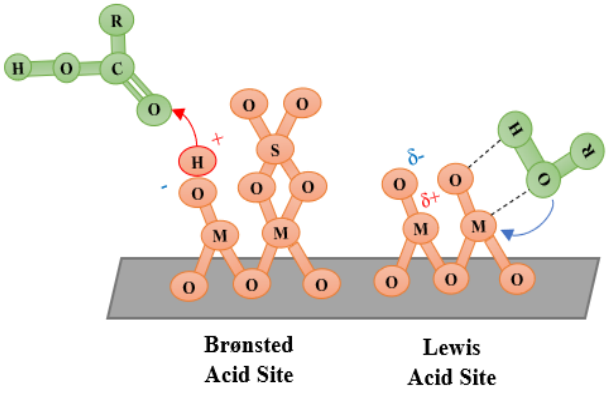

Figure 3. Lewis and Brønsted acid sites.

2.2. Production of Solid Acid Nanomaterials

Acidic nanocatalysts can be developed through either a "top-down" or a "bottom-up" methodology [43]. Top-down methods begin with bulk material and gradually refine downwards into an engineered nanoscale structure, whereas bottom-up approaches begin at nanoscale and progressively build upwards to obtain a desirable catalytic nanostructure. A variety of synthesis routes have been explored in past literature, as summarized in Figure 4 below. It is important to carefully consider which production strategy to utilize, since biodiesel yield depends on sufficient catalyst surface area and porosity to ensure effective mass transport of reactants towards active sites [44]. The stability of active sites against leaching, poisoning and other deactivation effects can also be influenced by the synthesis route performed, impacting the maximum recyclability that is achievable [45]. Unfortunately, it is difficult to predict which approach will be optimal or what the best synthesis conditions should be ahead of time; therefore, significant work continues to explore how best to synthesize optimal nanocatalysts with both impressive reactivity and reusability.

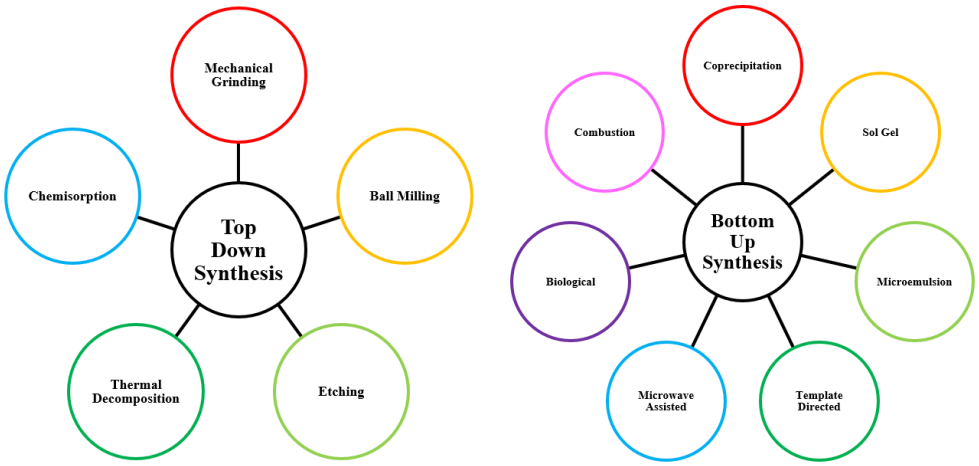

Figure 4. Methodologies for nanocatalyst production.

As discussed previously, nanomaterials can be functionalized post-synthesis to introduce new catalytically active functional groups, either to increase existing reactivity or provide an optimal balance of both Lewis and Brønsted acidity. On a solid surface, it is possible to achieve superacidity, defined as an acid strength greater than 100% pure sulfuric acid. This is often denoted via a Hammett acidity (H_0) function value below −12 [46], and can be experimentally determined through the use of standard indicator dyes [47].

Inclusion of sulfur-based compounds onto the catalyst surface by reacting with concentrated sulfuric acid [48], chlorosulfonic acid [49] or ammonium sulfate [50] have all been well-explored methods of increasing resilience to FFA impurities, with acid loading and strength influenced by the type of sulfation agent selected. The addition of organic alkyl or aromatic groups has also been explored by using propylsulfonic and toluenesulfonic acids [51,52]. Introduction of less polar organic acid sites has been observed to reduce deposition from polar FFA impurities and hence improve reusability; however, at the potential cost of reduced activity by weaker acid strength.

Sulfation not only increases Brønsted acid behaviour, but can enhance the Lewis acidity of metal-based solid catalysts through the inductive effect, drawing even more electron density away from the metal cation and increasing the ability for electron pair acceptance to occur. The sulfate ion (SO_4^{2-}) can exist in a variety of forms: for sulfated metal oxides this includes a chelated, bridged, or free ion structure [53], as illustrated in Figure 5. The sulfate loading achieved can influence the Brønsted/Lewis ratio, with high loadings favouring polynuclear sulfate structures with more Brønsted sites present [54]. The total acid site density and Brønsted/Lewis ratio can be experimentally determined via techniques such as ammonia temperature programmed desorption (TPD) [55] and pyridine diffuse reflectance FTIR spectroscopy (DRIFTS) [38], respectively.

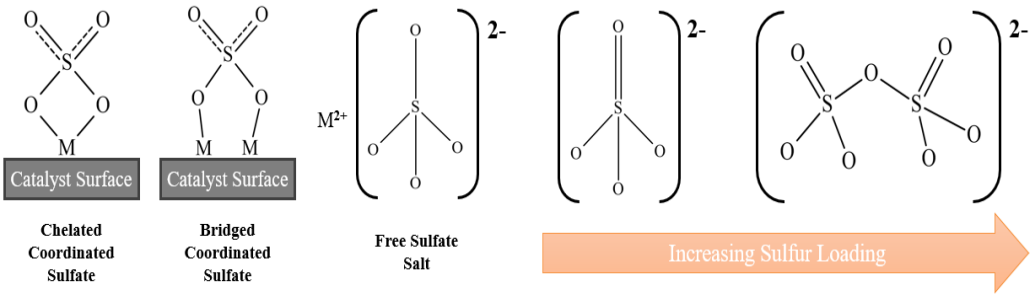

Figure 5. Sulfate structures on metal oxide materials.

After synthesis and acid functionalization, the superacidic solid is usually dried and calcinated at high temperatures. Alongside functionalization agent and synthesis route selected, these thermal treatments can also affect the acidity of the resulting catalyst. Drying is often performed to remove water and other volatiles introduced during synthesis, but can also influence acid strength by reducing the hydration of Brønsted acid sites [56]. Calcination then further removes leftover hydration and residual organic species alongside achieving a desirable crystallinity. It is important to note, however, that excessive calcination temperatures can lead to thermal decomposition of the sulfate active sites through the evolution of SO_x gases [39]. To avoid this, prior calcination steps should ideally be performed to set the desired metallic phase before lower temperature calcination of the sulfated nanocatalyst. TPD studies can also be utilised to determine a suitable calcination range that avoids sulfate loss. Too high a temperature can also lead to aggregation and reduced surface area [22], thereby impeding mass transfer to active sites and reducing reactivity.

A range of previous literature reviews [57–89] have summarised the use of various sulfated materials as part of a wider investigation into catalysis for biodiesel production. The following review section will now focus exclusively on recent developments of sulfated materials, focusing first on metal oxide-based nanocatalysts before porous silica and acidic carbon. In this review, nanocatalysts are defined as materials displaying either nanoparticle sizes, typically considered to be below 100 nm, or reactions that are catalysed within a confined highly porous nanoscale structure. Where reported, particle and pore sizes are displayed throughout in various summary tables arranged by date of publica-

tion. These tables also include key reaction and catalyst performance metrics, such as: alcohol to oil molar ratio (A:O), catalyst loading, reaction time and temperature, yield or conversion achieved, catalyst reusability, surface area, and acidity.

2.3. Acidic Nanocatalyst Development

A range of catalyst supports have been explored for biodiesel production, leading to the development of various sulfated acidic nanocatalysts. To date, materials based on sulfated metallic oxides generally show superior tolerance to feedstock impurities, making their application for cheap waste feeds such as WCO highly desirable. Some of these are explored in greater detail, providing various industrial uses, crystallographic structures and summaries of recent catalytic developments for biodiesel production.

2.3.1. Fe Oxide

Iron oxides see a diverse range of applications, for example, the production of durable dyes and paints to use in welding through the thermite reaction. Although many different types of iron oxide exist, the three most commonly explored forms for chemical catalysis are those of hematite (α-Fe_2O_3), maghemite (γ-Fe_2O_3) and magnetite (Fe_3O_4). The magnetic properties of these oxides are of particular interest, and Figure 6 illustrates the crystal structure of each respective oxide.

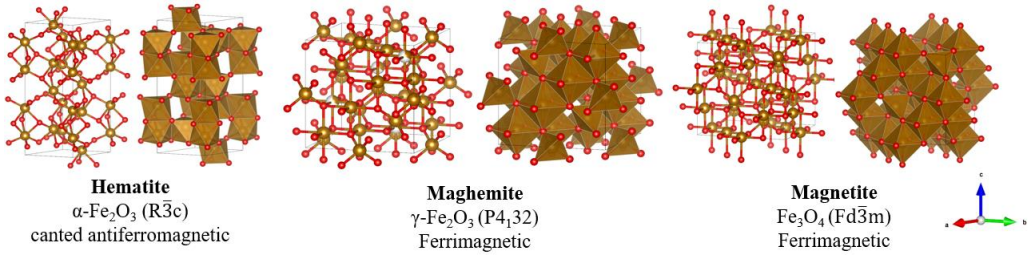

Figure 6. Crystallographic structure of common iron oxides.

Hematite is only very weakly magnetic—meanwhile, maghemite and magnetite are ferrimagnetic in nature and much more magnetically separable [90]. At the nanoscale, it is possible to create catalysts that display superparamagnetism, a desirable state in which external magnetic fields can induce magnetic separation with far greater susceptibility than typically expected for a paramagnetic material [91]. This allows for significantly enhanced maneuverability, and has been explored in the biomedical field for MRI imaging and targeted drug delivery [92]. The magnetic properties of these oxides have led to significant recent research into nanocatalysts that can be recovered post-reaction by the application of external magnetic fields. The potential opportunity for a rapid separation technique that easily facilitates nanomaterial regeneration and reuse is highly desirable. Although the Lewis acidic nature of iron oxides can be used for catalysing biodiesel production, surface functionalization is often performed to introduce new acidic functional groups, producing a more reactive and highly separable Fe oxide acidic nanocatalyst. A selection of recently developed sulfated Fe oxide nanocatalysts is summarised in Table 1.

Table 1. Summary of some Fe oxide sulfated catalysts.

Catalyst	Feedstock	A:O Ratio	Catalyst Loading (wt%)	Time (min)	T (°C)	Yield Y Conversion C	Reusability (Runs)	Particle Size (nm)	Pore Size (nm)	Surface Area (m^2/g)	Acidity (mmol/g)	Year	Ref.
FCHC-SO_3H	Oleic acid	15:1	4	180	80	96.7–84.3% Y	5	144	6.4	41.4	1.20	2018	[52]
SO_4/Mg/Al/Fe_3O_4	WCO	9:1	4	300	95	~98.5% Y	5	core: 20–150 shell: 5–15	6.5	123	2.35	2019	[93]
AC-Fe-SO_3Cl	PFAD	16:1	4	180	100	98.6–~79% C	6	45.21	8.8	20.4	29.5	2019	[94]

2.3.2. Ti Oxide

Titania enjoys a wide range of commercial application, such as: water and air purification systems, use as a white pigment, cosmetics and sunscreen, sensors, and self-cleaning films. Alongside being a widely researched photocatalyst, a desirable surface area combined with strong physical and chemical stability makes titania an excellent choice for a reactive catalyst support [95]. Sulfated titania has hence been widely studied as a solid acid catalyst for biodiesel production [78]. Titania exists in three main forms known as anatase, rutile and brookite, as displayed in Figure 7.

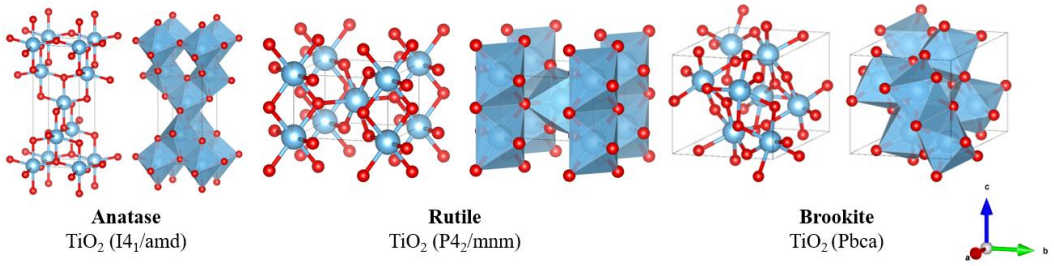

Figure 7. Crystallographic structure of common titanium oxides.

Of these three structures, anatase has been most widely explored for solid catalysis due to optimal surface area and strong interaction with other metallic oxide species, with rutile rarely achieving superior catalytic activity [96]. Anatase transforms to the more thermally stable rutile above calcination temperatures of approximately 600 °C, thereby restricting the maximum desirable calcination temperature when synthesizing a solid acid nanocatalyst. An overview of recent developments in sulfated titania-based nanocatalysis is given in Table 2.

Table 2. Summary of some Ti oxide-based sulfated catalysts.

Catalyst	Feedstock	A:O Ratio	Catalyst Loading (wt%)	Time (min)	T (°C)	Yield Y Conversion C	Reusability (Runs)	Particle Size (nm)	Pore Size (nm)	Surface Area (m^2/g)	Acidity (mmol/g)	Year	Ref.
SO_4^{2-}/ZrO_2–TiO_2/La^{3+}	Rapeseed oil fatty acids	1 mL/g	5	300	60	95–>90% C	5	-	-	-	-	2010	[97]
$TiO_2/SO_4^{2-}/(NH_4)_2SO_4$	Oleic acid	10:1	2	180	80	82.2% C	-	-	4.2	178	1.1	2010	[50]
TiO_2/SO_4^{2-}	Acetic acid 1.2 butanol	1.2 butanol	1.8 g	150	120	92.2–52.1% Y	4	8–10	12.9	121	0.79	2014	[48]
Sulfated Fe_2O_3/TiO_2	Soybean oil	20:1	15	120	100	~100–~80% C	4	89–103	-	16	-	2014	[39]
$Ti(SO_4)O$	WCO	9:1	1.5	180	75	97.1–94.12% Y	8	25	22.7	44.5	-	2016	[49]
$TiO_2/PrSO_3H$	WCO	15:1	4.5	540	60	98.3–94.16% Y	4	23.1	24.6	38.6	-	2017	[51]
SO_4/Fe-Al-TiO_2	WCO	10:1	3	150	90	96–>90% Y	10	<50	11.1	51	1.18	2017 – 2018	[38,98]
ZrO_2-TiO_2-SO_3H	Palmitic acid	20:1	5	240	100	93.1–85.1% Y	5	Length: 4000, Width: 100	-	32.5	1.9	2019	[99]

2.3.3. Zn Oxide

Zinc oxide has many important industrial applications, from rubber manufacturing, textiles, and pharmaceuticals, to specialized uses in electronics and photocatalysis [100,101]. As an amphoteric oxide, zinc oxide has been explored as both an acidic and basic catalytically active species for the production of biodiesel through transesterification and esterification pathways. Alongside the direct use of zinc oxide and in combination with other metallic oxides to form MMO materials, zinc oxide has been successfully sulfated to introduce Brønsted acidity.

The crystalline structure of zinc oxide commonly used for biodiesel production is that of a hexagonal wurtzite, shown above in Figure 8, since this form is most thermodynamically stable at ambient pressures. To produce a cubic form, pressures of around 9 GPa would be required, and degradation soon occurs when returned to ambient conditions [102]. Table 3 summarises different zinc oxide solid acid catalysts that have been used for biodiesel production.

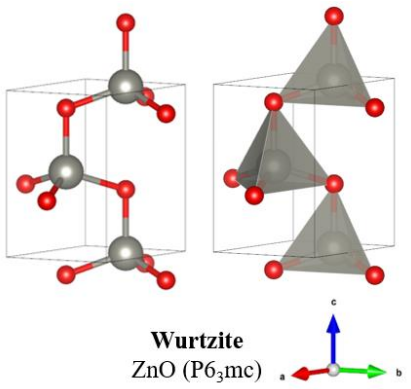

Figure 8. Crystallographic structure of zinc oxide.

Table 3. Summary of some Zn oxide-based sulfated catalysts.

Catalyst	Feedstock	A:O Ratio	Catalyst Loading (wt%)	Time (min)	T (°C)	Yield Y Conversion C	Reusability (Runs)	Particle Size (nm)	Pore Size (nm)	Surface Area (m^2/g)	Acidity (mmol/g)	Year	Ref.
ZnO	Pongamia oil	10:1	11.5	90	60	92% C	-	-	-	-	-	2005	[103]
SO_4^{2-}/ZnO	Soybean oil	6:1	4	240	65	80.2% Y	-	-	-	-	-	2015	[104]
SO_3H-$ZnAl_2O_4$	PFAD	9:1	1	60	120	94.65–67.29% Y	8	-	3.10	352.39	1.95	2016	[105]
ZnO-SO_3H	PFAD	9:1	2	90	120	95.6–>80% Y	6	-	3.16	305.62	1.72	2017	[55]

2.3.4. Zr Oxide

Zirconia is an important ceramic material, commonly used in fields such as dentistry, nuclear power, and catalysis, due to high mechanical and chemical resilience [106]. Similar to titania, the sulfation of zirconia to introduce Brønsted acidity has been widely explored as a solid acid nanocatalyst for biodiesel production. Unfortunately, while zirconia itself may be resilient, sulfated zirconia often suffers catalytic deactivation after a few runs via the leaching of sulfate sites [107,108]. In order to improve recyclability, recent studies have explored combining zirconia with other metal oxides to promote the stronger bonding of acid groups to the solid surface. Such MMO catalysts have successfully achieved much higher numbers of recycles before deactivation occurs. Zirconia is typically utilised in three major crystallographic forms, as shown below in Figure 9.

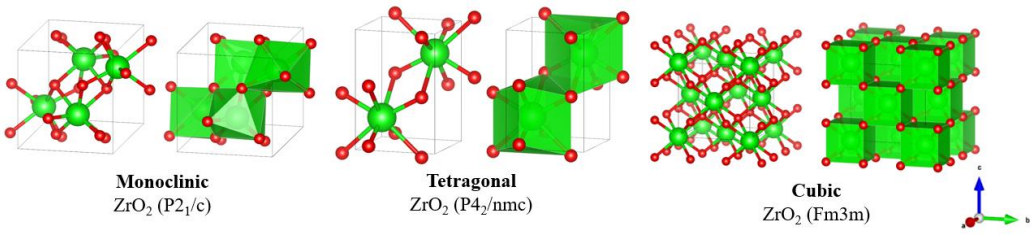

Figure 9. Crystallographic structure of common zirconium oxides.

The monoclinic phase is the largest crystal structure and most stable under ambient conditions. Through calcination and the introduction of other species, such as sulfate groups and metal oxides, desirable tetragonal structures can be stabilized. While similar can be achieved with cubic forms, catalysts explored for biodiesel production predominantly focus on monoclinic and tetragonal structures. Tetragonal zirconia is highly desirable, because acidity and therefore catalytic activity are enhanced for sufficiently large tetragonal to monoclinic ratios [109]. This is due to how basic surface hydroxyls interact differently with each crystal structure [110]. A summary of developments over time for solid acid zirconia-based catalysts is provided in Table 4.

Table 4. Summary of some Zr oxide-based sulfated catalysts.

Catalyst	Feedstock	A:O Ratio	Catalyst Loading (wt%)	Time (min)	T (°C)	Yield Y Conversion C	Reusability (Runs)	Particle Size (nm)	Pore Size (nm)	Surface Area (m^2/g)	Acidity (mmol/g)	Year	Ref.
SO_4^{2-}/ZrO_2	Palm kernel oil	6:1	1	60	60	90.3% Y	1	-	-	-	-	2006	[108]
Sulfated ZrO_2	Soybean oil	20:1	5	60	120	98.6% Y	1	-	-	126	-	2008	[111]
Sulfated ZrO_2	Neem oil	9:1	1	120	65	94% C	-	$2–3 \times 10^4$	-	-	-	2010	[112]
SO_4^{2-}/ZrO_2–B_2O_3–Fe_3O_4	Acetic acid	-	-	240	100	98.2–96.7% Y	5	-	-	-	-	2010	[113]
Fe_2O_3-MnO-SO_4^{2-}/ZrO_2	WCO	20:1	3	240	180	~96.5% Y	6	11.5–21	-	1.39×10^{-6}	4.32 A 1.52 B	2015	[114]
Sulfated ZrO_2	Oleic acid	10:1	10	240	150	81.3% Y	-	-	5.9	65.8	0.414	2017	[109]
FeMn-Sulfated ZrO_2	Tannery waste sheep fat	15:1	8	300	65	98.7–>90% Y	5	-	-	-	-	2020	[115]
SO_4^{2-}/ZrO_2-CeO_2	Jatropha oil	15.3:1	8	60	140	87.4–85.4% C	5	10	-	83.4	-	2021	[116]

2.3.5. Silica-Supported Nanocatalysts

Porous silica has been extensively explored in a wide range of fields, from drug delivery and pharmaceuticals to separation technology and chemical catalysis. Figure 10 below shows some of the many porous silica/aluminosilicate materials currently being explored.

Figure 10. Various silica-based porous materials in development.

As an inert catalyst support, silica facilitates the production of materials with impressively large surface areas and highly porous, nanoscale channel networks. The ability to tune pore size distribution and functionalize the surface with a wide range of metal oxides and sulfated groups has produced many solid acid catalysts for biodiesel production. A summary of some of these recent developments over time is included in Table 5. As per IUPAC definitions, pore sizes can be classed as either microporous (<2 nm diameter), mesoporous (2–50 nm) or macroporous (>50 nm) [117]. Macropores facilitate high mass transfer rates of reactants into the internal nanoscale structure, while meso/micropores provide substantial reaction surface area for catalysis to occur. Since triglyceride molecules are typically 2–6 nm in molecular diameter [23,51], only esterification can occur in micropores,

whereas both transesterification and esterification are achievable in mesoporous nanochannels, as illustrated in Figure 11.

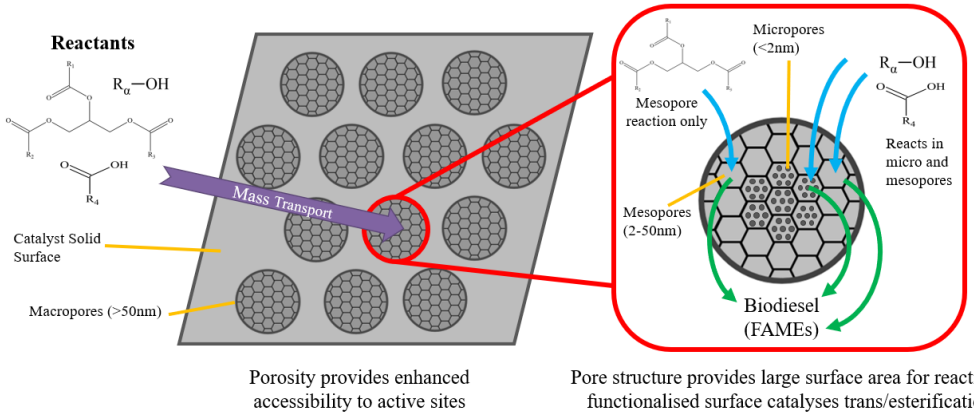

Figure 11. Mass transport and chemical reaction in porous solid acids.

Table 5. Summary of some silica-supported sulfated catalysts.

Catalyst	Feedstock	A:O Ratio	Catalyst Loading (wt%)	Time (min)	T (°C)	Yield Y Conversion C	Reusability (Runs)	Particle Size (nm)	Pore Size (nm)	Surface Area (m^2/g)	Acidity (mmol/g)	Year	Ref.
$SO_4^{2-}/TiO_2/SiO_2$	Acetic acid	-	-	-	120	91.4% C	-	-	-	550	-	2003	[118]
SBA-15-SO_3H-Pr	Untreated beef tallow	20:1	10	120	120	92–84% C	2	-	4.8	920	0.91	2006	[119]
SBA-15-SO_3H	Palmitic acid	30:1	0.05 g	360	60	50% Y	-	-	3.9	938	0.22	2010	[120]
TMS Capped/arene-SO_3H/SBA-15	Palm oil	20:1	6	240	140	~95% Y	3	-	8.3	533	1.04	2010	[121]
SBA-15-SO_3H	Palmitic acid	30:1	0.05 g	360	60	33.5% C	-	-	13.8	531	0.19	2012	[122]
KIT-6/C-SO_3H	Maleic anhydride	6:1	0.2 g	1800	-	~60% Y	4	-	11	590	3.0	2012	[123]
$SO_4^{2-}/TiO_2/SiO_2$	WCO	20:1	10	180	120	77–74.3% C	2	-	2.85	457	-	2013	[124]
SO_4^{2-}/La_2O_3/HZSM-5	Oleic acid	5:1	10	420	100	~100% C	1	17–150 × 10^3	5.2–120	217	-	2013	[125]
Fe/Fe_3O_4/SiO_2/APTES-$NHSO_2H$	Glyceryl trioleate	8:1	5	1200	100	100–>90% C	5	60	-	-	0.48	2015	[45]
SO_4^{2-}/Zr-SBA-15	WCO	40:1	3	180	160	98.5–~80% C	6	-	3.27–5.47	271	-	2015	[126]
SZ/MgO/SBA-15	Tributyrin	60 cm^3 meOH, 5 mmol TG	34	180	60	40% C	-	-	4–350	350	0.13 A 0.045 B	2020	[127]

2.3.6. Functionalised Carbon Nanocatalysts

Instead of the sulfated metal oxides or porous inert silicas, carbon-based solid acid nano catalysts can also be developed through treatment with strong acids. Compared with metals, acidic carbon materials can be produced more economically and with a lower overall environmental impact, since a wide variety of readily available waste biomasses can be converted into catalyst supports [128]. However, issues facing solid carbon acid catalysts, such as reduced activity, deactivation, and poor thermal stability, still need to

be addressed in order to improve catalytic performance and recyclability [129]. For the most challenging production of biodiesel from impure feedstocks such as WCO, metal oxide technology will therefore likely remain superior. New studies continue to address such problems however, with recent developments shown in Table 6.

Table 6. Summary of some functionalized carbon catalysts.

Catalyst	Feedstock	A:O Ratio	Catalyst Loading (wt%)	Time (min)	T (°C)	Yield Y Conversion C	Reusability (Runs)	Particle Size (nm)	Pore Size (nm)	Surface Area (m^2/g)	Acidity (mmol/g)	Year	Ref.
CNF-Ar-SO_3H	Triolein	10:1	0.75 g	240	120	~72% Y	4	-	-	-	0.62	2013	[130]
SO_3H-GO	Oleic acid	0.1 mol/g	5	240	100	97.6–74% C	3	-	3.8	437	-	2016	[129]
PC-SO_3H	Acetic acid	10:1	10	600	75	94–80% C	3	0.2–0.4 × 10^5	17	140	1.58	2016	[131]
S-MWCNTs	Trilaurin	20:1	3.7	60	150	97.8–~85% Y	2	Length: 0.5–2 × 10^3 Width: 20–30	5–35	199	-	2017	[132]
Al^{3+}/SO_4^{2-}/MWCNT	Oleic acid	12:1	0.9	420	65	95–81.1% C	8	Width: ~25	-	-	-	2017	[56]
Graphene-SO_3H	Palm oil	20:1	10	600	100	~98% Y	4	-	-	-	1.75	2017	[133]

Nanoscale carbon can be engineered bottom-up through the creation of nanofiber, nanotube, or graphene structures; or developed top-down from converting sugars, algae residues, and biomasses into solid catalysts. A range of carbon support types have been studied, as summarised in Figure 12. Plant biomasses often contain both carbon and metallic species [134], and mixing metal oxides with carbon has been explored to exploit differences in surface behaviour. The more non-polar carbon advantageously draws in other hydrophobic molecules such as triglycerides towards catalytic sites, whilst impeding polar species such as water that might lead to deactivation [135].

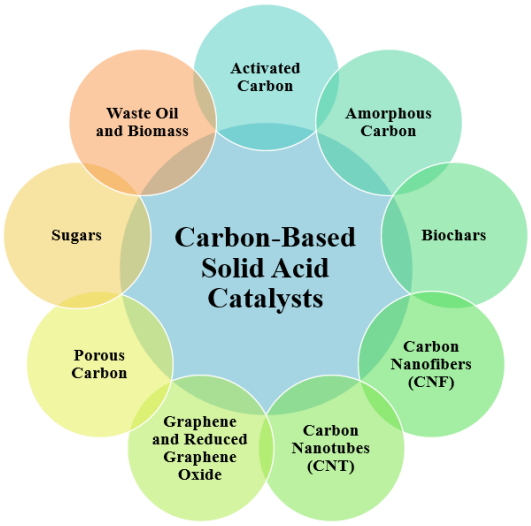

Figure 12. Types of carbon-based catalysts developed.

3. Challenges and Opportunities

The field of sulfated solid acid nanocatalysis for biodiesel production continues to see the development of new materials at pace, with a range of different approaches that

each present various strengths and weaknesses. Because each study utilizes vastly different reaction conditions, types of solid acid material and synthesis approaches, an overall comment on the direction of progress over time is difficult to make. However, there remains several key issues throughout the years that have yet to be adequately addressed in the literature and will need to be faced before commercial viability can be achieved. In order for sulfated nanocatalysts to be used at scale, they must be suitable for application into current biorefineries and potential future reactor technology.

Modern biorefineries have been designed with process intensification in mind, reducing complexity, wastage, and energy requirements, and thereby improving economic and environmental aspects of biodiesel production. An important side effect of this is the use of continuous reaction technology. In comparison, unfortunately most studies from the literature instead focus on batch reaction schemes. While this is acceptable for initial explorations of catalyst performance, it is not a true demonstration of how catalysts would be utilised commercially. Unlike batch reactors, continuous systems can achieve a more consistent biodiesel product, ensuring international fuel standards such as EN14214 and ASTM D6751 [4] are met with little variation in quality. Higher throughputs are also attainable, producing sufficient biodiesel to meet a forecasted ever-growing market demand. By transitioning towards assessing performance in lab-scale continuous reaction and separation schemes, sulfated acid materials would be tested in a more industrially relevant scenario. Particularly notable successes could then warrant scale up to pilot studies and may even lead to eventual full-scale application.

The design of a continuous reactor to test newly developed catalysts would depend on knowing the kinetic parameters for the reaction. Regrettably, only a few studies have performed kinetic trials to determine such information. Presented in Table 7 is the kinetic data reported for sulfated solid acid catalysts explored in this review. The turnover frequency (TOF) can be understood as a measure of active site efficiency, and is defined as the number of passes through the catalytic cycle per unit time. Computing a value of TOF can be difficult for sulfated acidic catalysts, due to the presence of a wide variety of catalytically active sites that must be accounted for, as well as the challenge of calculating an accurate reaction rate [136]. TOF can be calculated from estimating the turnover number (TON), defined as the ratio of moles reactant to moles catalyst, and adjusted based on the yield achieved [137]. This is illustrated in Equations (1) and (2). The use of chemisorption techniques may prove superior however, such as the previously discussed ammonia-TPD method for identifying medium and strong acid site densities. With the total loading of acidic sites measured, a lower bound value for the true TOF can hence be calculated [138]. Values of TOF range from 10^{-2} to 10^{1} min^{-1} for recently developed catalysts.

$$TON = \frac{moles\ reactant}{moles\ catalyst} \times yield \quad (1)$$

$$TOF = \frac{TON}{Reaction\ Time} \quad (2)$$

Reaction order is found to be unitary, which could be predicted since methanol is almost always added in large excess of the stoichiometric ratio, shifting the equilibrium towards biodiesel production as described by Le Chatelier's principle. Therefore, for sufficiently high alcohol to oil ratios, biodiesel production could be reasonably expected to be a pseudo first-order reaction. Activation energy lies mainly within the 30–80 kJ/mol range often observed for biodiesel production. It is recommended that kinetic studies to be undertaken, to better inform future application studies.

Table 7. Kinetic parameters of some acidic nanocatalysts.

Catalyst	T (°C)	TOF (min^{-1})	Ea (kJ/mol)	K (min^{-1})	n	Year	Reference
SBA-15/sulfonic acid	60	0.13–0.58	-	-	-	2010	[120]

KIT-6/C-SO_3H	-	0.57	-	-	-	2012	[123]
SBA-15/sulfonic acid	60	0.20–2.00	-	-	-	2012	[122]
SO_4^{2-}/La_2O_3/HZSM-5	100	-	44	-	1	2013	[125]
CNF-Ar-SO_3H	120	0.32	-	-	-	2013	[130]
SO_3H-GO	100	-	13	0.921	1	2016	[129]
S-MWCNTs	150	-	72	0.0498	1	2017	[132]
Fe_3O_4-Chitosan-Hollow-Chitosan-SO_3H	80	-	38	0.0173	1	2018	[52]

The major advantage of sulfated acidic catalysts compared to solid bases is a superior tolerance to impurities such as FFA and water, reducing deactivation effects and avoiding the issue of soap formation via saponification. While many studies have demonstrated successful esterification and resilience to trial FFA, such as oleic and palmitic acid, it is important to demonstrate successful simultaneous esterification and transesterification when using realistic, economical, and readily available feedstocks also. Table 8 summarises reported catalytic performance when using WCO as one such feedstock with sulfated solid acid nanocatalysts.

Table 8. Summary of some acidic nanocatalysts using cheap WCO feedstock.

Catalyst	A:O Ratio	Catalyst Loading (wt%)	Time (min)	T (°C)	Yield Y Conversion C	Reusability (Runs)	Particle Size (nm)	Pore Size (nm)	Surface Area (m^2/g)	Acidity (mmol/g)	Year	Ref.
SO_4^{2-}/TiO_2-SiO_2	20:1	10	180	120	77% C	1	-	2.85	457	-	2013	[124]
Fe_2O_3-MnO-SO_4^{2-}/ZrO_2	20:1	3	240	180	~96.5% Y	6	11.5–21	-	1.39×10^{-6}	4.32 A 1.52 B	2015	[114]
SO_4^{2-}/Zr-SBA-15	40:1	3	180	160	98.5–80% C	6	-	3.27–5.47	271	-	2015	[126]
$Ti(SO_4)O$	9:1	1.5	180	75	97.1–94.12% Y	8	25	22.7	44.5	-	2016	[49]
$TiO_2/PrSO_3H$	15:1	4.5	540	60	98.3–94.16% Y	4	8.2–42	24.6	38.6	-	2017	[51]
SO_4^{2-}/Fe-Al-TiO_2	10:1	3	150	90	96–>90% Y	10	<50	11.1	51	1.18	2017 2018	[38,98]
SO_4^{2-}/Mg-Al-Fe_3O_4	9:1	4	300	95	~98.5% Y	5	25–165	6.5	123	2.35	2019	[93]

Recyclability remains a challenge, despite new catalysts being regularly developed. Deactivation can occur due to a variety of reasons and different regeneration approaches have been tried to extend activity, as illustrated in Figure 13. Washing and drying steps can be used to remove organic depositions that poison the catalyst surface which, followed by recalcination, can also help to remove organic impurities. Recalcination may also be required should loss of crystallinity have occurred during reaction. While it is important that leaching be minimized to ensure adherence to biodiesel specifications, small losses of metal cations and acidic sulfate groups will unavoidably occur over extended use. Therefore, chemical treatments could be utilised to replace catalytically active species and restore activity. As has been noted by other literature studies [139], spent catalytic material is often not characterised to determine how material properties change post-reaction, thereby regrettably missing the opportunity to learn more about the specific deactivation mechanisms dominating activity loss. It is encouraged that future studies more regularly determine the primary cause of deactivation, so as to inform development of superior catalysts designed to reduce such effects. While recent work by Gardy et al. [38,98] using SO_4^{2-}/Fe-Al-TiO_2 achieved high yield over an impressive 10 consecutive runs with impure WCO feed, there continues to be a strong desire to further extend catalyst

lifespan without expending significant cost in material regeneration. Work involving sulfated zirconia as part of an MMO catalyst has led to encouraging improvements in recyclability and retention of sulfate groups. Likewise, while it may be that sulfated metal oxides are more suitable for conversion of cheap raw feedstocks than sulfated carbon, recent work such as the Al^{3+}/SO_4^{2-}/MWCNT catalyst synthesized by Shu et al. [56] could challenge that theory. An impressive eight consecutive uses could be performed, although it would have been preferable to see WCO used instead of model FFA oleic acid. It is hoped that similar improvements may be made over time with other types of sulfated solid acids.

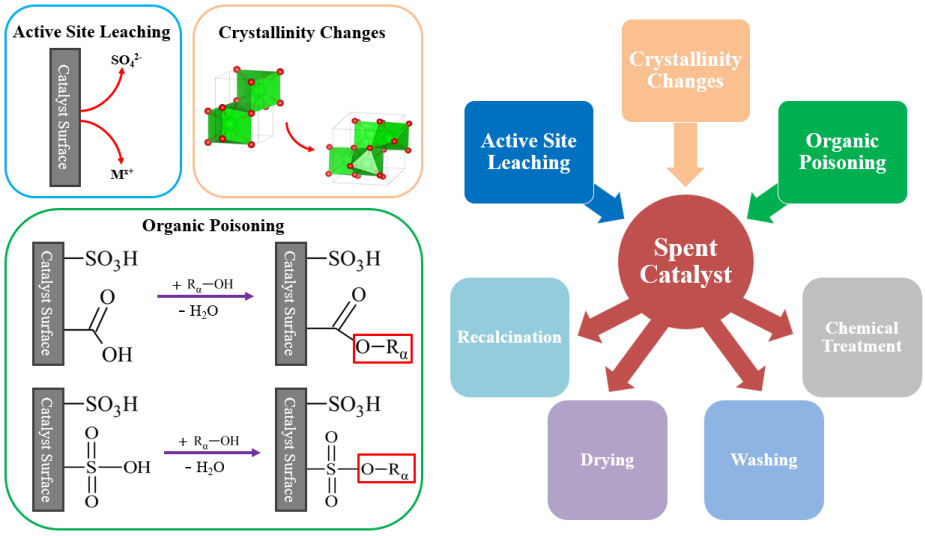

Figure 13. Catalytic deactivation routes and regeneration approaches.

The continuous separation and regeneration of catalytic material could also be explored further, for instance performing the reacidification of lost sulfate groups and washing as independent continuous steps, aiming towards an eventual completely closed loop system. It is often noted how external magnetic fields could simplify nanocatalyst recovery by inclusion of magnetic species such as iron oxides into sulfated acids. Thus far, however, there is a lack of work demonstrating the successful continuous magnetic separation within the application of biodiesel production.

Alongside demonstrating the successful reaction of sulfated solid acids in continuous reaction schemes with realistic impure feedstocks such as WCO, the catalytic material itself must also be produced via a rapid, simple, consistent, and economical synthesis route at the industrial scales required. The choice of synthesis route selected can considerably impact properties of the final obtained catalyst, as demonstrated by various papers that reported catalysts outside typical nanomaterial sizes. For example, issues such as insufficient size reduction during milling or over functionalization can lead to excessively large particle size, while excessive calcination temperature or calcination time can lead to aggregation and particle size growth, hindering nanoscale properties. Pore blockage and surface area reduction may also occur from using suboptimal ratios of metal species during synthesis. Therefore, alongside producing new types of catalyst, studies that synthesize a previously reported catalyst under optimized or entirely different reaction routes would be of interest.

As previously discussed, different functionalization agents can impact surface acidity and hydrophobicity, potentially leading to improved biodiesel yield or tolerance to deactivation effects. Figure 14 illustrates some of the sulfated acidic species that have been previously explored. New ways to introduce sulfated species onto a nanoscale metal, silica or carbon structure may be of novel research interest. To synthesize a sufficient catalyst

required for full scale usage, continuous production technologies will need to be investigated. Recent work by Mahin and Torrente-Murciano [140] demonstrated the continuous synthesis of Fe/Fe_3O_4 core-shell nanoparticles followed by surface functionalization with oleic acid, achieving a production rate of 2.6 g/h. Despite being far too low for commercial application, such studies suggest that continuous sulfated solid acid nanocatalyst production might be possible, and could be investigated further in future work. The requirement for calcination and drying steps would likely restrict lab studies to a semi-continuous synthesis scheme, but it would be important to demonstrate a nanocatalyst can be produced continuously with consistent structural properties and chemical performance before scaling up to commercial operation.

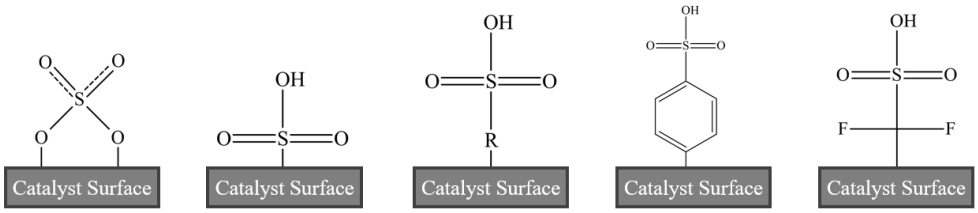

Figure 14. Sulfated functional groups explored to date.

Considering the various types of sulfated catalysts that have been explored thus far, in general, sulfated metal oxide nanomaterials have demonstrated the greatest tolerance for impure feedstocks to date. Significant work has been carried out to reach this point of high performance, and it is difficult to gauge how much more improvement could be realistically achieved from acidic sulfated MMO materials alone. Therefore, further advancements within this area are likely to be found through developing novel bifunctional nanomaterials, utilizing the resilience of strong acid sites to protect and sustain the high reactivities of vulnerable basic groups. Carbon functionalized nanomaterials still require further exploration and will need to demonstrate improvements in impurity resilience. Although some studies using acidic carbon nanotubes show impressive recyclability, more work will be required to justify whether these materials are suitable for cheap feedstocks such as WCO. Should a highly active and resilient nanocatalyst be achieved from waste biomass carbon sources, this could have the potential to be highly environmentally and economically desirable. It is likely that new research avenues will continue to be explored in developing an even greater range of sulfated nanocatalysts for biodiesel production, with the lead author currently investigating a novel nanoparticle design specifically intended for WCO feedstock. The technology readiness level of sulfated solid acid nanoscale catalysts is currently between 3–4; however, it is hoped that with renewed efforts to address remaining challenges and provide evidence that commercial viability is attainable, larger pilot scale studies may commence within the near future.

4. Conclusions

The world is increasingly realizing the urgent need to reduce GHG emissions, yet despite renewed global attention, the transportation sector is witnessing emission rate increases faster than any other sector. Decarbonization of personal transportation has been difficult to date, and unfortunately even with improvements in electric vehicle technologies there remains a substantial legacy population of combustion vehicles to provide fuel for, especially in less economically developed countries. Biodiesel offers a route to reduced emissions; however, its production from cheap waste feedstocks such as WCO demands especially resilient catalyst technology. Sulfated solid acidic catalysts are more easily separable and recyclable compared to traditional homogenous routes, and can handle the increased FFA content of cheap impure feeds without pre-treatment, but typically suffer reduced kinetics compared to base catalysis.

Switching to nanoscale sulfated acidic catalysts could achieve enhanced reactivities while remaining separable and resilient; therefore, much work continues to develop a range of materials based on metal oxides, mixed metal oxides, porous silica, and carbon through various top-down and bottom-up synthesis approaches. Recent progress over time within the field has been summarized by type of sulfated solid acid nanocatalyst, and while it is clear that improvements are steadily being made alongside the development of new catalytic materials, there remains significant challenges to overcome before such catalysts could be considered commercially viable.

Reaction tests need to be demonstrated in continuous reaction schemes, and newly developed catalysts should have kinetic parameters more regularly quantified to assist reactor design. The direct use of impure feedstocks such as WCO should be prioritized to confirm performance in realistic feeds. Separation and catalyst recovery also need to be trialled in a continuous scheme, in particular the use of external fields to separate magnetic sulfated nanoparticles. Although there have been notable improvements to the reusability of sulfated zirconia and acidic carbon, more work could better understand and mitigate against deactivation effects, as well as developing and optimizing catalyst regeneration approaches. Synthesis routes can have a significant impact on catalyst performance, and should continue to be explored, alongside varying functionalization agents to introduce desirable surface acidity and hydrophobicity. The potential for new methods of functionalization and the inclusion of sulfur-containing acidic species could also be investigated. To ensure sufficient catalytic material is available for industrial use, synthesis approaches will need to be demonstrated either via continuous process or in larger batches, without negatively affecting performance. Despite significant research to date, sulfated acid nanocatalysts have yet to fully demonstrate commercial viability in realistic industrial scenarios using cheap and impure feedstocks. It is hoped that through further work focused on paving a road towards pilot studies, such materials will see commercial adoption in modern biorefineries, moving society towards a brighter and lower carbon future.

Author Contributions: Conceptualization, J.G. and B.L.; resources, J.G. and B.L.; writing—original draft preparation, B.L.; writing—review and editing, J.G. and A.H.; supervision, J.G. and A.H.; project administration, A.H. All authors have read and agreed to the published version of the manuscript.

Funding: B.L. acknowledges financial support from the EPSRC Doctoral Training Partnership (EP/T517860/1). J.G. thanks the MDPI publisher for the APC funding.

Conflicts of Interest: The authors declare no conflict of interest.

Nomenclature:

A:O	Alcohol to Oil ratio
APTES	(3-Aminopropyl)-triethoxysilane
COK	Centrum voor Oppervlaktechemie en Katalyse (Centre for Research Chemistry and Catalysis)
COP26	2021 United Nations Climate Change Conference
DRIFTS	Diffuse Reflectance FTIR Spectroscopy
FAME	Fatty Acid Methyl Ester
FFA	Free Fatty Acid
FSM	Folded Sheets Mesoporous Material
FTIR	Fourier Transform Infrared Spectroscopy
GHG	Green House Gases
HMM	Hiroshima Mesoporous Material
HPA	Hetero Poly Acid
HZSM	H+ Zeolite Socony Mobil
KCC	KAUST Catalyst Centre
KIT	Korea advanced Institute of science and Technology
MCM	Mobil Composition of Matter
MSNP	Mesoporous Silica NanoParticles

MMO	Mixed Metal Oxide
PFAD	Palm Fatty Acid Distillate
SBA	Santa Barbara Amorphous
TMS	Tri Methyl Silane
TOF	Turn Over Frequency
TON	Turn Over Number
TPD	Temperature Programmed Desorption
TUD	Technische Universiteit Delft (Delft Technical University)
WCO	Waste Cooking Oil

References

1. COP26. 2021. Available online: https://ukcop26.org/ (accessed on 24 January 2022).
2. DoT. *Zero Emission Vehicles Transition Council: 2022 Action Plan*; Department of Transport: UK, 2021.
3. Sharma, A.; Shapps, G. Government Takes Historic Step towards Net-Zero with End of Sale of New Petrol and Diesel Cars by 2030. 2020. Available online: https://www.gov.uk/government/news/government-takes-historic-step-towards-net-zero-with-end-of-sale-of-new-petrol-and-diesel-cars-by-2030 (accessed on 30 June 2021).
4. *D6751—20a*; Standard Specification for Biodiesel Fuel Blend Stock (B100) for Middle Distillate Fuels. ASTM International: West Conshohocken, PA, USA, 2020.
5. *D7467—20a*; Standard Specification for Diesel Fuel Oil, Biodiesel Blend (B6 to B20). ASTM International: West Conshohocken, PA, USA, 2020.
6. Sheehan, J.; Camobreco, V.; Duffield, J.; Graboski, M.; Shapouri, H. *An Overview of Biodiesel and Petroleum Diesel Life Cycles*; National Renewable Energy Laboratory: Golden, CO, USA, 1998.
7. McLaughlin, D.W. Land, food, and biodiversity. *Conserv. Biol.* **2011**, *25*, 1117–1120.
8. Gui, M.M.; Lee, K.T.; Bhatia, S. Feasibility of edible oil vs. non-edible oil vs. waste edible oil as biodiesel feedstock. *Energy* **2008**, *33*, 1646–1653.
9. Rehan, M.; Gardy, J.; Demirbas, A.; Rashid, U.; Budzianowski, W.; Pant, D.; Nizami, A. Waste to biodiesel: A preliminary assessment for Saudi Arabia. *Bioresour. Technol*. **2018**, *250*, 17–25.
10. Morales, G.; Bautista, L.F.; Melero, J.A.; Iglesias, J.; Sánchez-Vázquez, R. Low-grade oils and fats: Effect of several impurities on biodiesel production over sulfonic acid heterogeneous catalysts. *Bioresour. Technol*. **2011**, *102*, 9571–9578.
11. Park, Y.-M.; Lee, D.-W.; Kim, D.-K.; Lee, J.-S.; Lee, K.-Y. The heterogeneous catalyst system for the continuous conversion of free fatty acids in used vegetable oils for the production of biodiesel. *Catal. Today* **2008**, *131*, 238–243.
12. Aransiola, E.; Ojumu, T.; Oyekola, O.; Madzimbamuto, T.; Ikhu-Omoregbe, D. A review of current technology for biodiesel production: State of the art. *Biomass Bioenergy* **2014**, *61*, 276–297.
13. Al-Qaysi, K.; Nayebzadeh, H.; Saghatoleslami, N.; Gardy, J. Effect of the loading of di-and tri-valent metal cations on the performance of sulfated silica-titania nano-catalyst in the esterification reaction. *J. Nanostruct.* **2021**, *11*, 221–235.
14. Luque, R.; Lovett, J.C.; Datta, B.; Clancy, J.; Campelo, J.M.; Romero, A.A. Biodiesel as feasible petrol fuel replacement: A multidisciplinary overview. *Energy Environ. Sci*. **2010**, *3*, 1706–1721.
15. Samios, D.; Pedrotti, F.; Nicolau, A.; Reiznautt, Q.; Martini, D.; Dalcin, F. A transesterification double step process—TDSP for biodiesel preparation from fatty acids triglycerides. *Fuel Process. Technol*. **2009**, *90*, 599–605.
16. Ghadge, S.V.; Raheman, H. Biodiesel production from mahua (*Madhuca indica*) oil having high free fatty acids. *Biomass Bioenergy* **2005**, *28*, 601–605.
17. Kawashima, A.; Matsubara, K.; Honda, K. Development of heterogeneous base catalysts for biodiesel production. *Bioresour. Technol.* **2008**, *99*, 3439–3443.
18. Dai, Y.-M.; Li, Y.-Y.; Lin, J.-H.; Kao, I.-H.; Lin, Y.-J.; Chen, C.-C. Applications of M_2ZrO_2 (M = Li, Na, K) composite as a catalyst for biodiesel production. *Fuel* **2021**, *286*, 119392.
19. Sulaiman, N.F.; Abu Bakar, W.A.W.; Toemen, S.; Kamal, N.M.; Nadarajan, R. In depth investigation of bi-functional, Cu/Zn/γ-Al_2O_3 catalyst in biodiesel production from low-grade cooking oil: Optimization using response surface methodology. *Renew. Energy* **2019**, *135*, 408–416.
20. Watkins, R.S.; Lee, A.F.; Wilson, K. Li–CaO catalysed tri-glyceride transesterification for biodiesel applications. *Green Chem*. **2004**, *6*, 335–340.
21. Naderi, F.; Nayebzadeh, H. Performance and stability assessment of Mg-Al-Fe nanocatalyst in the transesterification of sunflower oil: Effect of Al/Fe molar ratio. *Ind. Crop. Prod*. **2019**, *141*, 111814.
22. Xue, B.-J.; Luo, J.; Zhang, F.; Fang, Z. Biodiesel production from soybean and Jatropha oils by magnetic $CaFe_2O_4$–$Ca_2Fe_2O_5$-based catalyst. *Energy* **2014**, *68*, 584–591.
23. López, D.E.; Goodwin, J.G.; Bruce, D.A.; Furuta, S. Esterification and transesterification using modified-zirconia catalysts. *Appl. Catal. A Gen.* **2008**, *339*, 76–83.
24. Banković–Ilić, I.B.; Miladinović, M.R.; Stamenković, O.S.; Veljković, V.B. Application of nano CaO–based catalysts in biodiesel synthesis. *Renew. Sustain. Energy Rev.* **2017**, *72*, 746–760.

25. Rahimi, T.; Kahrizi, D.; Feyzi, M.; Ahmadvandi, H.R.; Mostafaei, M. Catalytic performance of MgO/Fe_2O_3-SiO_2 core-shell magnetic nanocatalyst for biodiesel production of *Camelina sativa* seed oil: Optimization by RSM-CCD method. *Ind. Crops Prod.* **2021**, *159*, 113065.
26. You, Y.; Zheng, M.; Jiang, D.; Li, F.; Yuan, H.; Zhai, Z.; Ma, L.; Shen, W. Boosting supercapacitive performance of ultrathin mesoporous $NiCo_2O_4$ nanosheet arrays by surface sulfation. *J. Mater. Chem. A* **2018**, *6*, 8742–8749.
27. Cagno, V.; Gasbarri, M.; Medaglia, C.; Gomes, D.; Clement, S.; Stellacci, F.; Tapparel, C. Sulfonated nanomaterials with broad-spectrum antiviral activity extending beyond heparan sulfate-dependent viruses. *Antimicrob. Agents Chemother.* **2020**, *64*, 02001–02020.
28. Narasimharao, K.; Malik, M.A.; Mokhtar, M.M.; Basahel, S.N.; Al-Thabaiti, S.A. Iron oxide supported sulfated TiO_2 nanotube catalysts for NO reduction with propane. *Ceram. Int*. **2014**, *40*, 4039–4053.
29. Sekewael, S.J.; Pratika, R.A.; Hauli, L.; Amin, A.K.; Utami, M.; Wijaya, K. Recent progress on sulfated nanozirconia as a solid acid catalyst in the hydrocracking reaction. *Catalysts* **2022**, *12*, 191.
30. Karatzos, S.; Van Dyk, J.S.; McMillan, J.; Saddler, J. Drop-in biofuel production via conventional (lipid/fatty acid) and advanced (biomass) routes. Part I. *Biofuels Bioprod. Biorefining* **2017**, *11*, 344–362.
31. SkyNRG. Sustainable Aviation Fuel—Technology. 2022. Available online: https://skynrg.com/sustainable-aviation-fuel/technology/ (accessed on 11 February 2022).
32. Kusdiana, D.; Saka, S. Methyl esterification of free fatty acids of rapeseed oil astreated in supercritical methanol. *J. Chem. Eng. Jpn.* **2001**, *34*, 383–387.
33. Kusdiana, D.; Saka, S. Two-step preparation for catalyst-free biodiesel fuel production: Hydrolysis and methyl esterification. *Appl. Biochem. Biotechnol. Part A Enzyme Eng. Biotechnol.* **2004**, *115*, 781–792.
34. Kusdiana, D.; Saka, S. Effects of water on biodiesel fuel production by supercritical methanol treatment. *Bioresour. Technol*. **2004**, *91*, 289–295.
35. Warabi, Y.; Kusdiana, D.; Saka, S. Biodiesel fuel from vegetable oil by various supercritical alcohols. *Appl. Biochem. Biotechnol. Part A Enzyme Eng. Biotechnol.* **2004**, *115*, 793–802.
36. Warabi, Y.; Kusdiana, D.; Saka, S. Reactivity of triglycerides and fatty acids of rapeseed oil in supercritical alcohols. *Bioresour. Technol*. **2004**, *91*, 283–287.
37. Boocock, D.G.; Konar, S.K.; Mao, V.; Sidi, H. Fast one-phase oil-rich processes for the preparation of vegetable oil methyl esters. *Biomass Bioenergy* **1996**, *11*, 43–50.
38. Gardy, J.; Osatiashtiani, A.; Céspedes, O.; Hassanpour, A.; Lai, X.; Lee, A.F.; Wilson, K.; Rehan, M. A magnetically separable SO_4/Fe-Al-TiO_2 solid acid catalyst for biodiesel production from waste cooking oil. *Appl. Catal. B Environ.* **2018**, *234*, 268–278.
39. Anuradha, S.; Raj, K.; Vijayaraghavan, V.R.; Viswanathan, B. Sulphated Fe_2O_3-TiO_2 catalysed transesterification of soybean oil to biodiesel. *Indian J. Chem.* **2014**, *53*, 1493–1499.
40. Ashok, A.; Ratnaji, T.; Kennedy, L.J.; Vijaya, J.J.; Pragash, R.G. Magnetically recoverable Mg substituted zinc ferrite nanocatalyst for biodiesel production: Process optimization, kinetic and thermodynamic analysis. *Renew. Energy* **2021**, *163*, 480–494.
41. Jamil, F.; Myint, M.T.Z.; Al-Hinai, M.; Al-Haj, L.; Baawain, M.; Al-Abri, M.; Kumar, G.; Atabani, A.E. Biodiesel production by valorizing waste Phoenix dactylifera L. Kernel oil in the presence of synthesized heterogeneous metallic oxide catalyst (Mn@MgO-ZrO_2). *Energy Convers. Manag.* **2018**, *155*, 128–137.
42. Pesaresi, L.; Brown, D.; Lee, A.; Montero, J.; Williams, H.; Wilson, K. Cs-doped $H_4SiW_{12}O_{40}$ catalysts for biodiesel applications. *Appl. Catal. A Gen.* **2009**, *360*, 50–58.
43. Liu, Y.; Mai, S.; Li, N.; Yiu, C.K.; Mao, J.; Pashley, D.H.; Tay, F.R. Differences between top-down and bottom-up approaches in mineralizing thick, partially demineralized collagen scaffolds. *Acta Biomater.* **2011**, *7*, 1742–1751.
44. Afsharizadeh, M.; Mohsennia, M. Catalytic synthesis of biodiesel from waste cooking oil and corn oil over zirconia-based metal oxide nanocatalysts. *React. Kinet. Mech. Catal.* **2019**, *128*, 443–459.
45. Wang, H.; Covarrubias, J.; Prock, H.; Wu, X.; Wang, D.; Bossmann, S.H. Acid-Functionalized magnetic nanoparticle as heterogeneous catalysts for biodiesel synthesis. *J. Phys. Chem. C* **2015**, *119*, 26020–26028.
46. Olah, G.A.; Laali, K.; Farooq, O. Chemistry in superacids. 6. Perfluoroalkanesulfonic acid-boron perfluoroalkanesulfonates: New superacid systems for generation of carbocations and catalysts for electrophilic transformations of hydrocarbons. *J. Org. Chem.* **1984**, *49*, 4591–4594.
47. Vassena, D.; Kogelbauer, A.; Prins, R. Potential routes for the nitration of toluene and nitrotoluene with solid acids. *Catal. Today* **2000**, *60*, 275–287.
48. Zhao, H.; Jiang, P.; Dong, Y.; Huang, M.; Liu, B. A high-surface-area mesoporous sulfated nano-titania solid superacid catalyst with exposed (101) facets for esterification: Facile preparation and catalytic performance. *New J. Chem.* **2014**, *38*, 4541–4548.
49. Gardy, J.; Hassanpour, A.; Lai, X.; Ahmed, M.H. Synthesis of $Ti(SO_4)O$ solid acid nano-catalyst and its application for biodiesel production from used cooking oil. *Appl. Catal. A Gen.* **2016**, *527*, 81–95
50. Ropero-Vega, J.L.; Aldana-Pérez, A.; Gómez, R.; Niño-Gómez, M.E. Sulfated titania [TiO_2/SO_4^{2-}]: A very active solid acid catalyst for the esterification of free fatty acids with ethanol. *Appl. Catal. A Gen.* **2010**, *379*, 24–29.
51. Gardy, J.; Hassanpour, A.; Lai, X.; Ahmed, M.H.; Rehan, M. Biodiesel production from used cooking oil using a novel surface functionalised TiO_2 nano-catalyst. *Appl. Catal. B Environ.* **2017**, *207*, 297–310.
52. Wang, A.; Li, H.; Pan, H.; Zhang, H.; Xu, F.; Yu, Z.; Yang, S. Efficient and green production of biodiesel catalyzed by recyclable biomass-derived magnetic acids. *Fuel Process. Technol.* **2018**, *181*, 259–267.

53. Noda, L.K.; de Almeida, R.M.; Probst, L.F.D.; Goncalves, N. Characterization of sulfated TiO_2 prepared by the sol–gel method and its catalytic activity in the n-hexane isomerization reaction. *J. Mol. Catal. A Chem.* **2005**, *225*, 39–46.
54. Noda, L.K.; de Almeida, R.M.; Goncalves, N.; Probst, L.F.D.; Sala, O. TiO_2 with a high sulfate content—Thermogravimetric analysis, determination of acid sites by infrared spectroscopy and catalytic activity. *Catal. Today* **2003**, *85*, 69–74.
55. Soltani, S.; Rashid, U.; Al-Resayes, S.I.; Nehdi, I. Sulfonated mesoporous ZnO catalyst for methyl esters production. *J. Clean. Prod.* **2017**, *144*, 482–491.
56. Shu, Q.; Tang, G.; Liu, F.; Zou, W.; He, J.; Zhang, C.; Zou, L. Study on the preparation, characterization of a novel solid Lewis acid Al^{3+}-SO_4^{2-}/MWCNTs catalyst and its catalytic performance for the synthesis of biodiesel via esterification reaction of oleic acid and methanol. *Fuel* **2017**, *209*, 290–298.
57. Lotero, E.; Liu, Y.; Lopez, D.E.; Suwannakarn, K.; Bruce, A.D.A.; Goodwin, J.J.G. Synthesis of biodiesel via acid catalysis. *Ind. Eng. Chem. Res.* **2005**, *44*, 5353–5363.
58. Melero, J.A.; van Grieken, R.; Morales, G. Advances in the synthesis and catalytic applications of organosulfonic-functionalized mesostructured materials. *Chem. Rev.* **2006**, *106*, 3790–3812.
59. Dias, J.M.; Alvim-Ferraz, M.C.; Almeida, M.F.; Rivera-Utrilla, J.; Sanchez-Polo, M. Waste materials for activated carbon preparation and its use in aqueous-phase treatment: A review. *J. Environ. Manag.* **2007**, *85*, 833–846.
60. Melero, J.A.; Iglesias, J.; Morales, G. Heterogeneous acid catalysts for biodiesel production: Current status and future challenges. *Green Chem.* **2009**, *11*, 1285–1308.
61. Math, M.C.; Kumar, S.P.; Chetty, S.V. Technologies for biodiesel production from used cooking oil—A review. *Energy Sustain. Dev.* **2010**, *14*, 339–345.
62. Chouhan, A.P.S.; Sarma, A.K. Modern heterogeneous catalysts for biodiesel production: A comprehensive review. *Renew. Sustain. Energy Rev.* **2011**, *15*, 4378–4399.
63. Semwal, S.; Arora, A.K.; Badoni, R.P.; Tuli, D.K. Biodiesel production using heterogeneous catalysts. *Bioresour. Technol.* **2011**, *102*, 2151–2161.
64. Sharma, Y.C.; Singh, B.; Korstad, J. Advancements in solid acid catalysts for ecofriendly and economically viable synthesis of biodiesel. *Biofuels Bioprod. Biorefining* **2011**, *5*, 69–92.
65. Borges, M.E.; Díaz, L. Recent developments on heterogeneous catalysts for biodiesel production by oil esterification and transesterification reactions: A review. *Renew. Sustain. Energy Rev.* **2012**, *16*, 2839–2849.
66. Okoronkwo, M.; Galadima, A.; Leke, L. Advances in biodiesel synthesis: From past to present. *Elixir Appl. Chem.* **2012**, *43*, 6924–6945.
67. Lee, A.F.; Bennett, J.A.; Manayil, J.C.; Wilson, K. Heterogeneous catalysis for sustainable biodiesel productionviaesterification and transesterification. *Chem. Soc. Rev.* **2014**, *43*, 7887–7916.
68. Su, F.; Guo, Y. Advancements in solid acid catalysts for biodiesel production. *Green Chem.* **2014**, *16*, 2934–2957.
69. Lee, A.F.; Wilson, K. Recent developments in heterogeneous catalysis for the sustainable production of biodiesel. *Catal. Today* **2015**, *242*, 3–18.
70. Zhai, Y.; Zhu, Z.; Dong, S. Carbon-based nanostructures for advanced catalysis. *ChemCatChem* **2015**, *7*, 2806–2815.
71. Hanif, M.A.; Nisar, S.; Rashid, U. Supported solid and heteropoly acid catalysts for production of biodiesel. *Catal. Rev.* **2017**, *59*, 165–188.
72. Nigatu Gebremariam, S.; Marchetti, J.M. Biodiesel production technologies: Review. *AIMS Energy* **2017**, *5*, 425–457.
73. Soltani, S.; Rashid, U.; Al-Resayes, S.I.; Nehdi, I.A. Recent progress in synthesis and surface functionalization of mesoporous acidic heterogeneous catalysts for esterification of free fatty acid feedstocks: A review. *Energy Convers. Manag.* **2017**, *141*, 183–205.
74. Tran, D.-T.; Chang, J.-S.; Lee, D.-J. Recent insights into continuous-flow biodiesel production via catalytic and non-catalytic transesterification processes. *Appl. Energy* **2017**, *185*, 376–409.
75. Xiong, X.; Yu, I.K.M.; Cao, L.; Tsang, D.C.; Zhang, S.; Ok, Y.S. A review of biochar-based catalysts for chemical synthesis, biofuel production, and pollution control. *Bioresour. Technol.* **2017**, *246*, 254–270.
76. Kumar, D.; Sharma, S.; Srivastava, N.; Shukla, S.; Gaurav, K. Advancement in the utilization of nanocatalyst for transesterification of triglycerides. *J. Nanosci. Technol.* **2018**, *4*, 374–379.
77. Bahuguna, A.; Kumar, A.; Krishnan, V. Carbon-support-based heterogeneous nanocatalysts: Synthesis and applications in organic reactions. *Asian J. Org. Chem.* **2019**, *8*, 1263–1305.
78. Carlucci, C.; Degennaro, L.; Luisi, R. Titanium dioxide as a catalyst in biodiesel production. *Catalysts* **2019**, *9*, 75.
79. Gardy, J.; Rehan, M.; Hassanpour, A.; Lai, X.; Nizami, A.-S. Advances in nano-catalysts based biodiesel production from non-food feedstocks. *J. Environ. Manag.* **2019**, *249*, 109316.
80. Nayak, S.N.; Bhasin, C.P.; Nayak, M.G. A review on microwave-assisted transesterification processes using various catalytic and non-catalytic systems. *Renew. Energy* **2019**, *143*, 1366–1387.
81. Quah, R.V.; Tan, Y.H.; Mubarak, N.; Khalid, M.; Abdullah, E.; Nolasco-Hipolito, C. An overview of biodiesel production using recyclable biomass and non-biomass derived magnetic catalysts. *J. Environ. Chem. Eng.* **2019**, *7*, 103219.
82. Thangaraj, B.; Solomon, P.R.; Muniyandi, B.; Ranganathan, S.; Lin, L. Catalysis in biodiesel production—A review. *Clean Energy* **2019**, *3*, 2–23.
83. Wong, K.Y.; Ng, J.-H.; Chong, C.T.; Lam, S.S.; Chong, W.T. Biodiesel process intensification through catalytic enhancement and emerging reactor designs: A critical review. *Renew. Sustain. Energy Rev.* **2019**, *116*, 109399.

84. Bano, S.; Ganie, A.S.; Sultana, S.; Sabir, S.; Khan, M.Z. Fabrication and optimization of nanocatalyst for biodiesel production: An overview. *Front. Energy Res.* **2020**, *8*, 350.
85. Vasić, K.; Podrepšek, G.H.; Željko, K.; Leitgeb, M. Biodiesel production using solid acid catalysts based on metal oxides. *Catalysts* **2020**, *10*, 237.
86. Lowe, B.; Ahmad, A; Gardy, J.; Hassanpour, A. Nanomaterials used in biorefineries: Types, properties, and synthesis methods. In *Nanotechnology for Biorefinery*; Ingle, A.P., Ed.; Elsevier: Amsterdam, The Netherlands, 2022.
87. Lowe, B.; Gardy, J.; Wu, K.; Hassanpour, A. Mixed metal oxide catalysts. In *Biodiesel Production: Feedstocks, Catalysts and Technologies*; Rokhum, L., Ed.; John Wiley & Sons Ltd.: Hoboken, NJ, USA, 2022; Chapter 8, pp. 143–166.
88. Nguyen, H.; Nguyen, M.-L.; Su, C.-H.; Ong, H.; Juan, H.-Y.; Wu, S.-J. Bio-derived catalysts: A current trend of catalysts used in biodiesel production. *Catalysts* **2021**, *11*, 812.
89. Testa, M.L.; la Parola, V. Sulfonic acid-functionalized inorganic materials as efficient catalysts in various applications: A minireview. *Catalysts* **2021**, *11*, 1143.
90. Cornell, R.M.; Schwertmann, U. *The Iron Oxides: Structure, Properties, Reactions, Occurrences and Uses*; John Wiley & Sons: Hoboken, NJ, USA, 2003.
91. Huber, D.L. Synthesis, properties, and applications of iron nanoparticles. *Small* **2005**, *1*, 482–501.
92. Ali, A.; Zafar, H.; Zia, M.; ul Haq, I.; Phull, A.R.; Ali, J.S.; Hussain, A. Synthesis, characterization, applications, and challenges of iron oxide nanoparticles. *Nanotechnol. Sci. Appl.* **2016**, *9*, 49–67.
93. Gardy, J.; Nourafkan, E.; Osatiashtiani, A.; Lee, A.F.; Wilson, K.; Hassanpour, A.; Lai, X. A core-shell SO_4/Mg-Al-Fe_3O_4 catalyst for biodiesel production. *Appl. Catal. B Environ.* **2019**, *259*, 118093.
94. Ibrahim, N.A.; Rashid, U.; Taufiq-Yap, Y.H.; Yaw, T.C.S.; Ismail, I. Synthesis of carbonaceous solid acid magnetic catalyst from empty fruit bunch for esterification of palm fatty acid distillate (PFAD). *Energy Convers. Manag.* **2019**, *195*, 480–491.
95. Scirè, S.; Fiorenza, R.; Bellardita, M.; Palmisano, L. 21—Catalytic applications of TiO_2. In *Titanium Dioxide (TiO_2) and Its Applications*; Parrino, F., Palmisano, L., Eds.; Elsevier: Amsterdam, The Netherlands, 2021; pp. 637–679.
96. Bagheri, S.; Julkapli, N.M.; Hamid, S.B.A. Titanium dioxide as a catalyst support in heterogeneous catalysis. *Sci. World J.* **2014**, *2014*, 727496.
97. Li, Y.; Zhang, X.D.; Sun, L.; Zhang, J.; Xu, H.P. Fatty acid methyl ester synthesis catalyzed by solid superacid catalyst SO_4^{2-}/ZrO_2–TiO_2/La^{3+}. *Appl. Energy* **2010**, *87*, 156–159.
98. Gardy, J. Biodiesel Production from Used Cooking Oil Using Novel Solid Acid Catalysts. Ph.D. Thesis, University of Leeds, Leeds, UK, 2017.
99. Fan, M.; Si, Z.; Sun, W.; Zhang, P. Sulfonated ZrO_2-TiO_2 nanorods as efficient solid acid catalysts for heterogeneous esterification of palmitic acid. *Fuel* **2019**, *252*, 254–261.
100. Kumar, P.; Kumar, R.; Singh, R. Transition metals doped ZnO nanoparticles for 3D printing: A state of the art review and prospective applications. In *Reference Module in Materials Science and Materials Engineering*; Elsevier: Amsterdam, The Netherlands, 2020.
101. Borysiewicz, M.A. ZnO as a functional material, a review. *Crystals* **2019**, *9*, 505.
102. Sokolov, P.S.; Baranov, A.N.; Dobrokhotov, Z.V.; Solozhenko, V.L. Synthesis and thermal stability of cubic ZnO in the salt nanocomposites. *Russ. Chem. Bull.* **2010**, *59*, 325–328.
103. Karmee, S.K.; Chadha, A. Preparation of biodiesel from crude oil of Pongamia pinnata. *Bioresour. Technol.* **2005**, *96*, 1425–1429.
104. Istadi, I.; Anggoro, D.D.; Buchori, L.; Rahmawati, D.A.; Intaningrum, D. Active acid catalyst of sulphated zinc oxide for transesterification of soybean oil with methanol to biodiesel. *Procedia Environ. Sci.* **2015**, *23*, 385–393.
105. Soltani, S.; Rashid, U.; Yunus, R.; Taufiq-Yap, Y.H. Biodiesel production in the presence of sulfonated mesoporous $ZnAl_2O_4$ catalyst via esterification of palm fatty acid distillate (PFAD). *Fuel* **2016**, *178*, 253–262.
106. Keiteb, A.S.; Saion, E.; Zakaria, A.; Soltani, N. Structural and optical properties of zirconia nanoparticles by thermal treatment synthesis. *J. Nanomater.* **2016**, *2016*, 1913609.
107. Sun, Y.; Ma, S.; Du, Y.; Yuan, L.; Wang, S.; Yang, J.; Deng, F.; Xiao, F.S. Solvent-free preparation of nanosized sulfated zirconia with Brønsted acidic sites from a simple calcination. *J. Phys. Chem. B* **2005**, *109*, 2567–2572.
108. Jitputti, J.; Kitiyanan, B.; Rangsunvigit, P.; Bunyakiat, K.; Attanatho, L.; Jenvanitpanjakul, P. Transesterification of crude palm kernel oil and crude coconut oil by different solid catalysts. *Chem. Eng. J.* **2006**, *116*, 61–66.
109. Raia, R.Z.; Silva, L.; Marcucci, S.M.P.; Arroyo, P. Biodiesel production from *Jatropha curcas* L. oil by simultaneous esterification and transesterification using sulphated zirconia. *Catal. Today* **2017**, *289*, 105–114.
110. Jung, K.T.; Bell, A.T. The effects of synthesis and pretreatment conditions on the bulk structure and surface properties of zirconia. *J. Mol. Catal. A Chem.* **2000**, *163*, 27–42.
111. Garcia, C.M.; Teixeira, S.; Marciniuk, L.L.; Schuchardt, U. Transesterification of soybean oil catalyzed by sulfated zirconia. *Bioresour. Technol.* **2008**, *99*, 6608–6613.
112. Muthu, H.; Sathyaselvabala, V.; Varathachary, T.K.; Kirupha Selvaraj, D.; Nandagopal, J.; Subramanian, S. Synthesis of biodiesel from Neem oil using sulfated zirconia via tranesterification. *Braz. J. Chem. Eng.* **2010**, *27*, 601–608.
113. Guan, D.; Fan, M.; Wang, J.; Zhang, Y.; Liu, Q.; Jing, X. Synthesis and properties of magnetic solid superacid: SO_4^{2-}/ZrO_2–B_2O_3–Fe_3O_4. *Mater. Chem. Phys.* **2010**, *122*, 278–283.
114. Alhassan, F.H.; Rashid, U.; Taufiq-Yap, Y.H. Synthesis of waste cooking oil-based biodiesel via effectual recyclable bi-functional $Fe_2O_3MnOSO_4^{2-}$/ZrO_2 nanoparticle solid catalyst. *Fuel* **2015**, *142*, 38–45.

115. Booramurthy, V.K.; Kasimani, R.; Pandian, S.; Ragunathan, B. Nano-sulfated zirconia catalyzed biodiesel production from tannery waste sheep fat. *Environ. Sci. Pollut. Res.* **2020**, *27*, 20598–20605.
116. Li, X.F.; Ma, W.H.; Bao, G.R.; Lv, G.Q.; Wan, X.H.; Li, Q.J. Effect of preparation parameters on the catalytic performance of solid acid catalyst SO_4^{2-}/ZrO_2-CeO_2 in biodiesel production. *Fuel Cells* **2021**, *21*, 119–125.
117. Narayan, R.; Nayak, U.Y.; Raichur, A.M.; Garg, S. Mesoporous silica nanoparticles: A comprehensive review on synthesis and recent advances. *Pharmaceutics* **2018**, *10*, 118.
118. Yang, H.; Lu, R.; Wang, L. Study of preparation and properties on solid superacid sulfated titania–silica nanomaterials. *Mater. Lett.* **2003**, *57*, 1190–1196.
119. Mbaraka, I.K.; McGuire, K.J.; Shanks, B.H. Acidic mesoporous silica for the catalytic conversion of fatty acids in beef tallow. *Ind. Eng. Chem. Res.* **2006**, *45*, 3022–3028.
120. Dhainaut, J.; Dacquin, J.-P.; Lee, A.F.; Wilson, K. Hierarchical macroporous–mesoporous SBA-15 sulfonic acidcatalysts for biodiesel synthesis. *Green Chem.* **2010**, *12*, 296–303.
121. Melero, J.A.; Bautista, L.F.; Morales, G.; Iglesias, J.; Sánchez-Vázquez, R. Biodiesel production from crude palm oil using sulfonic acid-modified mesostructured catalysts. *Chem. Eng. J.* **2010**, *161*, 323–331.
122. Dacquin, J.P.; Lee, A.F.; Pirez, C.; Wilson, K. Pore-expanded SBA-15 sulfonic acid silicas for biodiesel synthesis. *Chem. Commun.* **2012**, *48*, 212–214.
123. Valle-Vigón, P.; Sevilla, M.; Fuertes, A.B. Sulfonated mesoporous silica–carbon composites and their use as solid acid catalysts. *Appl. Surf. Sci.* **2012**, *261*, 574–583.
124. Shao, G.; Sheikh, R.; Hilonga, A.; Lee, J.E.; Park, Y.-H.; Kim, H.T. Biodiesel production by sulfated mesoporous titania–silica catalysts synthesized by the sol–gel process from less expensive precursors. *Chem. Eng. J.* **2013**, *215–216*, 600–607.
125. Vieira, S.S.; Magriotis, Z.; Santos, N.A.; Saczk, A.A.; Hori, C.; Arroyo, P. Biodiesel production by free fatty acid esterification using Lanthanum (La^{3+}) and HZSM-5 based catalysts. *Bioresour. Technol.* **2013**, *133*, 248–255.
126. Yi, Q.; Zhang, J.; Zhang, X.; Feng, J.; Li, W. Synthesis of SO_4^{2-}/Zr-SBA-15 catalyst for the transesterification of waste cooking oil as a bio-flotation agent in coal flotation. *Fuel* **2015**, *143*, 390–398.
127. Isaacs, M.A.; Parlett, C.M.A.; Robinson, N.; Durndell, L.J.; Manayil, J.C.; Beaumont, S.K.; Jiang, S.; Hondow, N.S.; Lamb, A.C.; Jampaiah, D.; et al. A spatially orthogonal hierarchically porous acid–base catalyst for cascade and antagonistic reactions. *Nat. Catal.* **2020**, *3*, 921–931.
128. Malani, R.S.; Choudhury, H.A.; Moholkar, V.S. Chapter 13—Waste biorefinery based on waste carbon sources: Case study of biodiesel production using carbon based catalysts and mixed feedstocks of nonedible and waste oils. In *Waste Biorefinery*; Bhaskar, T., Pandey, A., Rene, E.R., Tsang, D.C.W., Eds.; Elsevier: Amsterdam, The Netherlands, 2020; pp. 337–378.
129. Mahto, T.K.; Jain, R.; Chandra, S.; Roy, D.; Mahto, V.; Sahu, S.K. Single step synthesis of sulfonic group bearing graphene oxide: A promising carbo-nano material for biodiesel production. *J. Environ. Chem. Eng.* **2016**, *4*, 2933–2940.
130. Stellwagen, D.R.; van der Klis, F.; van Es, D.S.; de Jong, K.P.; Bitter, J.H. Functionalized carbon nanofibers as solid-acid catalysts for transesterification. *ChemSusChem* **2013**, *6*, 1668–1672.
131. Tamborini, L.; Casco, M.; Militello, M.; Silvestre-Albero, J.; Barbero, C.; Acevedo, D. Sulfonated porous carbon catalysts for biodiesel production: Clear effect of the carbon particle size on the catalyst synthesis and properties. *Fuel Process. Technol.* **2016**, *149*, 209–217.
132. Guan, Q.; Li, Y.; Chen, Y.; Shi, Y.; Gu, J.; Li, B.; Miao, R.; Chen, Q.; Ning, P. Sulfonated multi-walled carbon nanotubes for biodiesel production through triglycerides transesterification. *RSC Adv.* **2017**, *7*, 7250–7258.
133. Nongbe, M.C.; Ekou, T.; Ekou, L.; Yao, K.B.; Le Grognec, E.; Felpin, F.-X. Biodiesel production from palm oil using sulfonated graphene catalyst. *Renew. Energy* **2017**, *106*, 135–141.
134. Gohain, M.; Laskar, K.; Paul, A.K.; Daimary, N.; Maharana, M.; Goswami, I.K.; Hazarika, A.; Bora, U.; Deka, D. Carica papaya stem: A source of versatile heterogeneous catalyst for biodiesel production and C–C bond formation. *Renew. Energy* **2020**, *147*, 541–555.
135. Poonjarernsilp, C.; Sano, N.; Tamon, H. Hydrothermally sulfonated single-walled carbon nanohorns for use as solid catalysts in biodiesel production by esterification of palmitic acid. *Appl. Catal. B Environ.* **2014**, *147*, 726–732.
136. Boudart, M. Turnover rates in heterogeneous catalysis. *Chem. Rev.* **1995**, *95*, 661–666.
137. Johansson Seechurn, C.C.C.; DeAngelis, A.; Colacot, T.J. Chapter 1 Introduction to new trends in cross-coupling. In *New Trends in Cross-Coupling: Theory and Applications*; The Royal Society of Chemistry: London, UK, 2015; pp. 1–19.
138. Spivey, J.J.; Roberts, G.W.; Goodwin, J.G., Jr.; Kim, S.; Rhodes, W.D. Turnover frequencies in metal catalysis: Meanings, functionalities and relationships. In *Catalysis: Volume 17*; Spivey, J.J., Roberts, G.W., Eds.; The Royal Society of Chemistry: London, UK, 2004; pp. 320–348.
139. Schüth, F.; Ward, M.D.; Buriak, J.M. Common pitfalls of catalysis manuscripts submitted to chemistry of materials. *Chem. Mater.* **2018**, *30*, 3599–3600.
140. Mahin, J.; Torrente-Murciano, L. Continuous synthesis of monodisperse iron@iron oxide core@shell nanoparticles. *Chem. Eng. J.* **2020**, *396*, 125299.